Available online at www.sciencedirect.com
SCIENCE DIRECT®
Polymer 44 (2003) 4599–4610
polymer
www.elsevier.com/locate/polymer

A Langevin-elasticity-theory-based constitutive equation for rubberlike networks and its comparison with biaxial stress–strain data. Part I

Bohumil Meissner*, Libor Matějka

Institute of Macromolecular Chemistry, Academy of Sciences of the Czech Republic, Heyrovský Square 2, 162 06 Prague 6, Czech Republic

Received 31 October 2002; received in revised form 29 April 2003; accepted 12 May 2003

Abstract

A structure-based constitutive equation for rubberlike networks is proposed. It is obtained by combining the Langevin-statistics-based theory of Arruda and Boyce (AB) with a term based on the first invariant of the generalized deformation tensor which follows from some theoretical treatments of the constraint effect. The combined (ABGI) four-parameter strain–energy function has been found to give (with the exception of the very-low strain region) a very good description (deviations $< 5–8\%$) of a representative selection of published biaxial stress–strain data obtained on networks of isoprene and natural rubbers at low and medium strains. For the description of biaxial extension data up to high strains, the concept of a strain-induced increase in the network mesh size (strain-dependent finite extensibility parameter) used previously for tensile strains, is shown to apply generally to all deformation modes. It also enables a prediction of the retraction behavior. Reasonable values were obtained for the network parameters; the exponent in the strain invariant assumes values at the higher limit of the Kaliske and Heinrich extended tube theory prediction or even somewhat outside the limits.

Keywords: Theory of rubber elasticity; Biaxial deformations; Experimental testing

1. Introduction

The problem of obtaining a sufficiently general description of the stress–strain behavior of rubberlike networks in different deformation modes was investigated in numerous papers (cf. reviews [1,2]). However, molecular theories published until recently gave only partial answers. The present paper explores the possibility of obtaining an as precise as possible description (with deviations less than 5%) of experimental stress–strain relations in a wide range of biaxial strain (preferably up to the break) using recently published constitutive equations based on molecular models [3–5].

Arruda and Boyce (AB) [3] improved the constitutive equation based on the Langevin elasticity theory using a new network model with its unit cell composed of eight chains. As in previous Langevin-type theories [1,6], two parameters are involved: the network-chain concentration and the network-chain length. At high strains, hardening due to finite extensibility effects is predicted while at low strains the behavior approaches the Gaussian one with the reduced stress (see Eq. (3)) becoming constant. Similarly to the older Langevin treatments, the AB theory does not deal with the phenomenon of the experimentally observed low-strain decrease in reduced tensile stress on increasing strain (the 'C2-effect', low-strain softening) and, therefore, the AB low-strain predictions cannot be expected to offer a quantitative data representation. In a recent review, Boyce and Arruda [7] suggest that combination of the Flory–Erman constrained junction model [8] for small stretches with the eight-chain model for the large stretch response and deformation state dependence would be expected to describe the data over the entire extensibility range more precisely than any of the models presented. They themselves made the first step towards this goal and obtained an improvement in describing the well-known Treloar data on a natural rubber network [9]. However, significant experiment–theory deviations still remain.

Equations predicting both low-strain softening and high-strain hardening were derived. That of Edwards and Vilgis is based on a slip-link concept [10]. It was tested experimentally by comparing with uniaxial [11] and biaxial [12] stress–strain measurements taken up to large strains.

* Corresponding author. Tel.: +420-296809384; fax: +420-296809410.
E-mail address: meissner@imc.cas.cz (B. Meissner).

0032-3861/03/$ - see front matter © 2003 Elsevier Science Ltd. All rights reserved.
doi:10.1016/S0032-3861(03)00411-7

The data description, though partly satisfactory, was unsuccessful in some important cases. Quite recently, biaxial data on solution-crosslinked poly(dimethylsiloxane) networks [13,14] have been compared with theoretical predictions. Of the five molecular theories tested, the Edwards-Vilgis model has shown the best ability to represent the stress–strain relations, moreover with the fitted parameter values in good accordance with those obtained from molecular considerations independently of mechanical testing [15,16]. However, the approach adopted includes disputable points which make the final conclusions less convincing [17]. If a more realistic initial assumption is used, the potential of the tube theories becomes apparent [17].

Another theory, recently published by Kaliske and Heinrich [4], has introduced an extended tube model that considers topological constraints and the limited chain extensibility of network chains both in unfilled and filled rubbers. In the resulting two-term strain energy function, W, the first part, W_A, is due to crosslinks and captures similar features as the AB equation and the crosslink term of the slip-link treatment. With two parameters (crosslinking degree and chain inextensibility parameter, δ), it predicts hardening at high strains. There is an important difference between the extended tube model theory [4] and the Langevin treatments [1,3,6]. For the end-to-end distance of a tube-like confined network chain, Kaliske and Heinrich [4] use 'the simplest model with the singularity in the chain entropy…instead of the more realistic inverse Langevin approximation'. In this respect, they follow Edwards and Vilgis [10]. Thus, the crosslink parts of the strain energy functions, W_A, calculated on the basis of the slip-link [10] and extended tube [4] models (and the stresses calculated from W_A, as well) are to be looked upon as mere phenomenological approximations of a conceivable rigorous structure-based tube treatment that would model the singularity in chain entropy using Langevin statistics and would probably lead to predictions similar to those of the AB equation. As shown in Appendix A, the degree of approximation included in the Kaliske–Heinrich W_A term [4] results in predictions that do not seem realistic. Kaliske and Heinrich [4] used their strain energy function to demonstrate a fairly good description of the well-known Treloar data. However, the arguments given above make their W_A function questionable and unsuitable for our purpose. The W_A-term in the Klüppel–Schramm theory [5] is of the same form as that of Kaliske and Heinrich.

The second part of the Kaliske–Heinrich strain–energy function, W_B, which is due to topological constraints, was formulated earlier and is given in a review [18] as Eq. (44) together with its structural background and interpretation. The function is written phenomenologically as based on the first invariant of the generalized deformation tensor (GI) [19,20] (hereinafter, generalized invariant, GI) and includes results of several theoretical models as special cases [4,5,18, 21–23].

In the present paper, experimental data are analyzed using a function where the crosslink term, W_A, is given by the rigorously derived structure-based Arruda and Boyce (AB) strain–energy density function [3] and the constraint term, W_B, is based on the first invariant of the generalized deformation tensor (GI) with its parameters having molecular basis in different tube theories. The proposed equation is designated by the ABGI code. It may be looked upon as a further attempt, following that of Boyce and Arruda [7], to interpret experimental behavior by combining the AB theory with a suitable treatment of the strain-softening effect.

2. Theoretical

2.1. Definitions

A homogenous biaxial deformation of an elastic and continuous body is assumed to take place in a rectangular coordinate system X_i ($i = 1, 2, 3$) which is taken along the principal axes of strain, σ_i ($i = 1, 2, 3$) being the principal (engineering) stresses (force per unit of undeformed area) and λ_i ($i = 1, 2, 3$) the principal stretch ratios. In a biaxial extension experiment with stresses along the directions 1, 2, the stress along the direction 3 is zero. At constant volume, $\lambda_3 = 1/\lambda_1\lambda_2$. If the equilibrium deformation behavior of an elastic material is described by a strain energy density function W (elastic free energy, constitutive equation) then the principal nominal (engineering) stresses σ_i ($i = 1, 2$) are obtained from the general relation

$$\sigma_i = \frac{\partial W}{\partial \lambda_i} - \frac{\lambda_3}{\lambda_i}\frac{\partial W}{\partial \lambda_3} \tag{1}$$

The stresses σ_1, σ_2, calculated in the Gaussian elasticity theory [1] can be written in the form

$$\sigma_1 = G(\lambda_1 - 1/\lambda_1^3\lambda_2^2); \qquad \sigma_2 = G(\lambda_2 - 1/\lambda_2^3\lambda_1^2) \tag{2}$$

The shear modulus G is proportional to the network density and absolute temperature. The reduced stresses $\sigma_{1,\mathrm{red}}$, $\sigma_{2,\mathrm{red}}$, are defined as the ratio of stress and of the corresponding Gaussian stretch ratio function:

$$\begin{aligned} \sigma_{1,\mathrm{red}} &= \sigma_1/(\lambda_1 - 1/\lambda_1^3\lambda_2^2); \\ \sigma_{2,\mathrm{red}} &= \sigma_2/(\lambda_2 - 1/\lambda_2^3\lambda_1^2) \end{aligned} \tag{3}$$

In the biaxial extension experiments, the dependences of stresses σ_1, σ_2, on the stretch ratio λ_2 are usually measured (and plotted) for different constant values of λ_1. This way of plotting data visually accentuates the scatter in the high-strain region while in the low-strain region, where the absolute values of deviations decrease, the relative deviations seem to be negligibly small. To avoid such disadvantage, we prefer the use of reduced stresses since their fluctuations approach the *relative* deviations. Further,

with λ_1 and λ_2 being interrelated, e.g. by

$$\lambda_2^2 = \lambda_1^b; \qquad (b\langle -1, +2\rangle, \lambda_1 \geq \lambda_2), \tag{4}$$

the stresses become functions of one stretch ratio only. Stress–strain dependences with $b = -1$ ($\lambda_2 = \lambda_3 = 1/\lambda_1^{0.5}$, $\sigma_2 = 0$, uniaxial extension, UE), $b = 2$ ($\lambda_2 = \lambda_1$, $\sigma_2 = \sigma_1$, equibiaxial extension, EBE,) and $b = 0$ ($\lambda_2 = 1$, longitudinal pure shear σ_1, PS1; transversal pure shear σ_2, PS2) are commonly measured directly. Stress–strain dependencies with other suitably chosen values of b (e.g. 0.5, 1, 1.5) can be obtained by interpolation from the dependences measured at constant values of one of the stretch ratios. In the following text, if λ_2 is related to λ_1 by Eq. (4), then subscript 1 in λ_1 is generally omitted.

2.2. The constraint part W_B

The phenomenological formulation of the W_B part of the strain–energy density function is given as [18]

$$W_B = G_e \frac{2I_1(n)}{n}; \qquad I_1(n) = \sum_i (\lambda_i^n - 1)/n \tag{5}$$

$I_1(n)$ is the first invariant of the generalized deformation tensor. In different tube theories, G_e is a constraint contribution to the modulus [18], which is proportional to the apparent concentration of elastically effective physical crosslinks arising from conformational constraints; the exponent in the strain invariant $n = -2\gamma\beta$; γ describes different constraint mechanisms while the β parameter, $0 \leq \beta \leq 1$, takes into account different extents of the constraint release processes [18]. In the Kaliske and Heinrich model [4], there is a non-affine relation between the lateral tube dimension and the local stretch ratio and $\gamma = +1/2$. β is an empirical fit parameter, correlating microscopic and macroscopic deformation (for affine deformation: $\beta = 1$). Thus, according to the Kaliske and Heinrich model, n should assume values between -1 and 0. In an earlier treatment of Heinrich and Straube [18,21] the result $\gamma = -1/4$, ($\beta = 1$), $n = +0.5$, was obtained under assumptions valid for high crosslink densities. In the model of Gaylord and Douglas [22], affinely deforming tubes with constant volume are considered and this leads to the prediction $\gamma = -1/2$, i.e. $n = +1$. These authors admit the possibility that γ (or, n) is not universal for all network structures and that other values may result from slightly modified models. They recommend treating γ (or, n) as an empirical parameter and determining its value for a variety of network systems. In the Klüppel and Schramm theory [5] of rubber elasticity and of stress softening of filler-reinforced elastomer systems, a generalized tube model is used with $\gamma = 1/2$, i.e. $n = -1$, which is the lowest value expected by the Kaliske and Heinrich treatment [4]. Klüppel and Schramm explored the possibility of replacing the Edwards–Vilgis approach to the finite network extensibility by the inverse Langevin approach but they rejected it on experimental grounds [5]. In the present paper, the Langevin approach is preferred on theoretical grounds.

Rubinstein and Panyukov [23] assume a non-affine deformation on smaller scales up to a certain 'affine' length which increases with elongation and decreases with compression. The calculated W_B is again proportional to entanglement concentration and has two equal parts, the first with $n = 1$ and the other with $n = -1$.

2.3. The ABGI equation

The constitutive equation for stress $\sigma_i (i = 1, 2)$ that we propose and denote by the ABGI code is obtained using the general Eq. (1) and the following derivatives

$$\frac{1}{2C_1}\frac{\partial W_A}{\partial \lambda_i} = \frac{\lambda_{cm}}{3\lambda_c} L^{-1}\left(\frac{\lambda_c}{\lambda_{cm}}\right)\lambda_i \tag{6}$$

$$\frac{1}{2C_2}\frac{\partial W_B}{\partial \lambda_i} = \frac{2\lambda_i^{n-1}}{n} \tag{7}$$

$$\lambda_c = (I/3)^{1/2}; \qquad I = \sum_i \lambda_i^2 \tag{8}$$

For $n = 0$,

$$\frac{1}{2C_2}\frac{\partial W_B}{\partial \lambda_i} = \frac{2\ln \lambda_i}{\lambda_i}$$

λ_c is the network-chain stretch ratio, i.e. the ratio of the deformed and undeformed chain end-to-end distances; in the Arruda and Boyce paper [3], λ_c is denoted as λ_{chain}. L^{-1} is the inverse Langevin function (the Langevin function $L(x) = \coth(x) - 1/x$), λ_{cm} is the hypothetical highest possible network chain stretch ratio (or, the finite extensibility parameter; the locking chain stretch ratio), which is predicted to be proportional to the square root of the network chain length expressed as the number, N, of statistical segments in the network chain:

$$\lambda_{cm} = N^{1/2} \tag{9}$$

$2C_1$ is the crosslink (network junction) contribution to the shear modulus. The shear modulus G in the original Arruda–Boyce equation is here replaced with $2C_1$; according to Arruda and Boyce, $G = \nu RT$, ν is the network chain density. The Kaliske-Heinrich parameter G_e is replaced with $2C_2$.

The proposed ABGI equation contains four adjustable parameters: C_1, C_2, λ_{cm}, n. The shear modulus G of the ABGI material is essentially determined by the elastic constants C_1, C_2. For a very large N, $G = 2C_1 + 2C_2$; with decreasing N, the contribution of finite extensibility to the stress has a non-zero positive value even at low strains and $G > 2C_1 + 2C_2$. The high-strain behavior is increasingly influenced by N which determines the square of the locking chain stretch, Eq. (9), and the maximum possible macroscopic stretch ratios which follow from $I_{max} = 3N$. For very large N and $n = -2$, the ABGI equation reduces to the Mooney–Rivlin equation [1,24,25]. With $n = +2$, the

constraints would contribute to the stress in the same manner as crosslinks. For some deformation modes, I is given by the following expressions:

uniaxial extension, UE

$$\lambda_2 = \lambda_3 = 1/\lambda_1^{1/2}: \quad I = \lambda_1^2 + 2/\lambda_1, \tag{10}$$

pure shear, PS $\quad \lambda_2 = 1; \lambda_3 = 1/\lambda_1: \quad I = \lambda_1^2 + 1 + 1/\lambda_1^2,$

equibiaxial extension, EBE

$$\lambda_2 = \lambda_1; \lambda_3 = 1/\lambda_1^2: \quad I = 2\lambda_1^2 + 1/\lambda_1^4$$

2.4. The ABGIL equation

In our previous paper [11], the JGC2 equation was defined as a combination of the Langevin-statistics-based James–Guth equation [6] with the C_2 term of the Mooney–Rivlin equation [24,25]. It was found to give a very good description of stress–strain data in uniaxial extension at low and medium stretch ratios. In conformity with previous evidence, the C_1 term was interpreted as being due to stable network junctions that receive contributions from both chemical crosslinks and some kind of stable–non-sliding–trapped entanglements. Stable junctions determine the concentration, ν_{eff}, and length, N, of elastically effective network chains. N is now the number of statistical segments in the chain between elastically effective network junctions of both chemical and stable entanglement type [11] and is a measure of the network mesh size.

High-strain deviations of the experimental behavior from the predictions of the JGC2 equation were observed and ascribed to topological changes leading to a strain-induced increase in the network mesh size and, as a result, to an increase in the finite extensibility parameter with the stretch ratio. The latter dependence found from comparison of the JGC2 equation with experimental data could be described by a simple power function [11] and the resulting set of equations was denoted as the JGC2L equation:

$$\sigma = 2C_1(\lambda_m/3)\{L^{-1}(\lambda/\lambda_m) - (1/\lambda^{3/2})L^{-1}(1/\lambda^{1/2}\lambda_m)\} + 2C_2(1 - 1/\lambda^3) \tag{11}$$

$$\lambda \le \lambda_a: \quad \lambda_m = \lambda_{m,a}, \tag{12}$$

$$\lambda > \lambda_a: \quad \lambda_m = \lambda_{m,a} + (\lambda_{m,b} - \lambda_{m,a})\{(\lambda - \lambda_a)/(\lambda_b - \lambda_a)\}^a$$

λ_m is the finite extensibility parameter, the locking stretch ratio. To avoid confusion with the numbering of axes, the subscripts 1,2 used previously [11] in λ_1, $\lambda_{m,1}$, etc. are replaced here with subscripts a, b, to obtain λ_a, $\lambda_{m,a}$, etc.

The phenomena observed in uniaxial extension are to be expected to manifest themselves in other deformation modes as well. Hence, the ABGI equation, Eqs. (6)–(8), has to be modified into a general ABGIL form by supplementing it with an equation expressing the dependence of the finite extensibility parameter on the state of strain. In view of the functional form of Eq. (6) and in analogy with the JGC2L equation, Eq. (12), the required relation is written as a power function dependence of the locking chain stretch ratio, λ_{cm}, on the chain stretch ratio, λ_c:

$$\lambda_c \le \lambda_{c,a}: \quad \lambda_{cm} = \lambda_{cm,a}, \tag{13}$$

$$\lambda_c > \lambda_{c,a}:$$

$$\lambda_{cm} = \lambda_{cm,a} + (\lambda_{cm,b} - \lambda_{cm,a})[(\lambda_c - \lambda_{c,a})/(\lambda_{c,b} - \lambda_{c,a})]^a$$

The ABGIL equation is thus given by Eqs. (6)–(8) and (13). For chain stretch ratios lower than $\lambda_{c,a}$, the finite extensibility parameter λ_{cm} is constant and equal to $\lambda_{cm,a}$. For chain stretch ratios higher than $\lambda_{c,a}$, the finite extensibility parameter increases with strain and at the

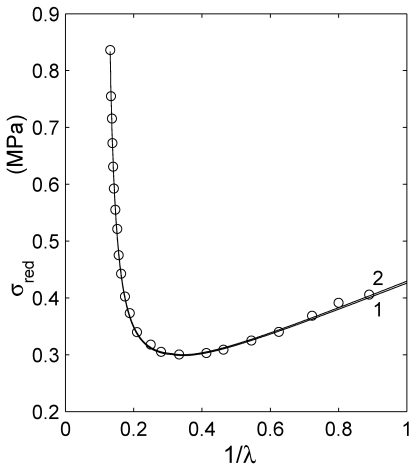

Fig. 1. Comparison of the Treloar uniaxial extension data on NR-1 (circles) with the equations JGC2L (curve 1) and ABGIL($n = -2$) (curve 2). Parameter values in Table 1. Mooney–Rivlin coordinates of reduced stress vs. reciprocal stretch ratio.

Table 1
Parameter values calculated from uniaxial extension data using equations JGC2L and ABGIL ($n = -2$)

JGC2L		ABGIL ($n = -2$)				
Parameter	NR-1	Parameter	NR-1	NR-2	NR-3	IR
C_1, MPa	0.092	C_1, MPa	0.092	0.070	0.132	0.127
C_2, MPa	0.118	C_2, MPa	0.118	0.112	0.120	0.082
λ_a	3.20	$\lambda_{c,a}$	1.903_1	–	1.795	–
$\lambda_{m,a}$	6.10	$\lambda_{cm,a}$	3.537_3	–	3.137_4	–
λ_b	7.60	$\lambda_{c,b}$	4.397_8	–	2.824_6	–
$\lambda_{m,b}$	8.31	$\lambda_{cm,b}$	4.806_1	3.80[a]	3.674_7	$>10^2$
a	1.03	a	1.03	–	1.35	–
$\sigma_{red,\lambda=1}$	0.426_2	$\sigma_{red,\lambda=1}$	0.429_5	0.370	0.522	0.418
C_2/C_1	1.28	C_2/C_1	1.28	1.60	0.91	0.65

[a] λ_{cm}.

chain stretch ratio $\lambda_{c,b}$, it attains the value of $\lambda_{cm,b}$. The method of determining the required parameters of the ABGIL equation is shown below.

3. Experimental testing

3.1. Uniaxial extension

Fig. 1 shows a Mooney–Rivlin plot of the Treloar data [1,9] obtained in uniaxial extension up to high strains on a natural rubber network NR-1 crosslinked with a high amount of sulfur. In such a network, possible effects of strain-induced crystallization are regarded as secondary in character, producing only minor modifications [1]. The Treloar uniaxial extension data were compared with the JGC2L equation and the parameter values (given in Table 1) were obtained in a manner described previously [11].

A special case of the ABGIL equation which follows from Eqs. (6)–(8) and (13) for $n = -2$ (designated by the ABGIL($n = -2$) code) combines the Arruda–Boyce equation with the C_2 term of the Mooney–Rivlin equation and is an analogy of the JGC2L equation in which the James–Guth equation is combined with the C_2 term. In accordance with our previous finding [11], the parameters $\lambda_{c,a}$, $\lambda_{cm,a}$, etc. of the ABGIL($n = -2$) equation can be calculated from the JGC2L λ_a, $\lambda_{m,a}$, etc. parameters by simply transforming them to the corresponding chain stretch ratio values using Eqs. (8) and (10) for the case of uniaxial extension: $\lambda_c = ((\lambda_1^2 + 2/\lambda_1)/3)^{1/2}$. This has been done for the Treloar network NR-1 and the calculated parameters are given in Table 1. The two curves drawn according to the JGC2L and ABGIL($n = -2$) equations, respectively, are compared in Fig. 1. A very small difference between them can be practically removed by slightly increasing C_2 of the JGG2L equation from 0.118 to 0.120 MPa. Thus, the JGC2L and ABGIL($n = -2$) equations are essentially equivalent for the description of the stress–elongation dependences and their parameters can easily be interconverted. Their fit to the experimental Treloar data in uniaxial extension shown in Fig. 1 is excellent with point-curve deviations being well below 5%.

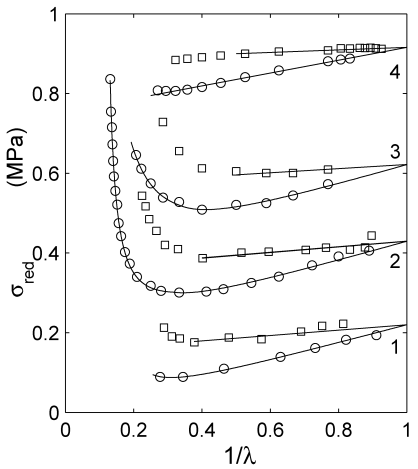

Fig. 2. Dependences of the experimental reduced uniaxial extension stress (circles) and reduced equibiaxial extension stress (squares) on reciprocal stretch ratio. 1-NR-2, vertical shift: −0.15; 2-NR-1; 3-NR-3, shift: +0.1; 4-IR, shift +0.5. UE data are compared with the ABGIL($n = -2$) curves drawn using parameter values given in Table 1. Straight lines are empirically fitted to the low-strain EBE data.

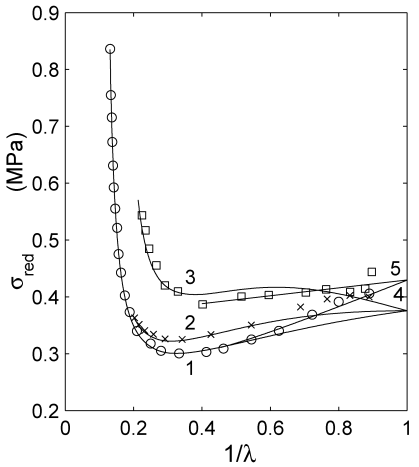

Fig. 3. Dependences of reduced uniaxial extension stress (circles, curve 1), pure shear stress (crosses, curve 2) and equibiaxial extension stress (squares, curve 3) on reciprocal stretch ratio, NR-1. Curves 1,2,3: ABGIL equation, $n = -0.2$, parameter values in Table 3, right. Curve 4: $n = -2$, parameter values in Table 1. Straight line 5: empirical fit to low-strain EBE data.

The parameters of the ABGIL($n = -2$) equation can, of course, be determined directly, without first comparing data with the JGC2L equation. An example of such a procedure is shown below for the general case of the ABGIL equation ($n > -2$).

The UE data on four networks are shown in the Mooney–Rivlin plot in Fig. 2 together with the EBE data. Both UE and EBE experimental dependences tend to be linear in the reciprocal stretch ratio region between ca. 0.5 and 0.9 and tend to extrapolate to the same zero-strain reduced stress, $\sigma_{red,\lambda=1}$. Straight lines are empirically fitted to the EBE data in the low-strain region. The UE data are described by ABGIL($n = -2$) curves which are drawn using parameter values given in Table 1. The degree of fit to all UE data is very good.

3.2. Biaxial extension, NR-1

Fig. 3 shows the Mooney–Rivlin plot of reduced stress vs. reciprocal stretch ratio of the Treloar stress–strain data [9] measured in uniaxial extension (UE), pure shear (PS) and equibiaxial extension (EBE). A linear extrapolation to $\lambda = 1$ of the low-strain reduced PS stress vs. reciprocal stretch ratio dependence also leads to a value close to that obtained from UE and EBE data.

As has been repeatedly shown [18], the parameter values of the Mooney–Rivlin equation determined from uniaxial extension data are not able to predict the biaxial extension

Table 2
Parameter values of the ABGI equation calculated from the low- and medium-strain UE, PS, EBE data

Parameter	NR-1
n	−0.20
C_1, MPa	0.109
C_2, MPa	0.075
λ_{cm}	4.2

behavior since an unrealistically large ratio of the equibiaxial to uniaxial stress is predicted. The same limitation is to be expected for the ABGIL($n = -2$) equation and to obtain a satisfactory description of a set of the UE, PS, EBE Treloar data using the ABGIL equation, a suitable value of $n > -2$ must be found. This, however, gives an ABGI prediction for the UE stress which is curved in the Mooney–Rivlin plot. The task of describing a *linear* experimental UE dependence by a theoretical *curve* is a sort of dilemma which has no unique solution and the result must be expected always to be more or less an approximation. In the following it will be shown that the approximation offered by the ABGIL equation is close to satisfactory and can be utilized for practical purposes.

In the first step, the low- and medium-strain biaxial extension data (UE, PS, EBE) were compared with the ABGI equation. The values of n and of the C_2/C_1 ratio were chosen to obtain a good fit to the experimental ratio of the equibiaxial to uniaxial stress and a calculated zero-strain reduced stress not very different from the value of the extrapolated experimental reduced stresses (0.425–0.43 MPa) given above. The resulting estimates of n, C_1, C_2 and λ_{cm} parameters of the ABGI equation are given in Table 2. They are used to draw the ABGI curve 1 in Fig. 4. The uniaxial experimental data (circles) are plotted in the coordinates of stress vs. chain stretch ratio $\lambda_{c,UE} = (\lambda_1^2 + 2/\lambda_1)^{1/2}/3^{1/2}$. Above the inflexion point, curve 1 increases more steeply than does the experimental dependence (points, curve 6) and this phenomenon is interpreted using the concept of a strain-dependent finite extensibility parameter (Eq. (13)). The method of determining parameter values of Eq. (13) is depicted in Fig. 4. Four additional curves 2–5 are drawn using increasing values of λ_{cm}. A most probable curve 6 is hand-fitted to the high-strain experimental UE points. From its intersections with curves 1–5 (or, preferably, with a larger number of such curves), one obtains a series of λ_{cm}, λ_c pairs (Table 3, left) which

Table 3
Parameter values of the ABGIL equation for the NR-1 network

Curve	Parameter	Fig. 4	Figs. 3,5,6	
	n	−0.20	−0.20	−0.40
	C_1, Mpa	0.109	0.109	0.109
	C_2, Mpa	0.075	0.075	0.068
	$\lambda_{c,a}$		2.289_3	2.178
	$\lambda_{cm,a}$		4.225_5	4.110_6
	$\lambda_{c,b}$		4.397_8	4.397_8
	$\lambda_{cm,b}$		4.886_7	4.875_2
	a		1.30	1.20
	$\sigma_{red,\lambda=1}$		0.375_7	0.362_2
	Δ, %		−12.5	−15.7
	C_2/C_1		0.79	0.62
	λ_{cm}	λ_c [a]		
1	4.225	(2.345)		
2	4.45	3.187_3		
3	4.60	3.632		
4	4.75	4.050		
5	4.89	4.406		

Δ : percent difference between $\sigma_{red,\lambda=1}$ calculated using ABGI($n > -2$) and the respective $\sigma_{red,\lambda=1}$ (given in Table 1) calculated using ABGI ($n = -2$).

[a] Chain stretch ratios for the intersections of curves 1–5 with the experimental curve 6. Parameters for the retraction curve 4 in Fig. 5: $C_1 = 0.100$ MPa, $C_2 = 0.075$ MPa, $\lambda_{cm} = 4.785$, tensile set 0.09.

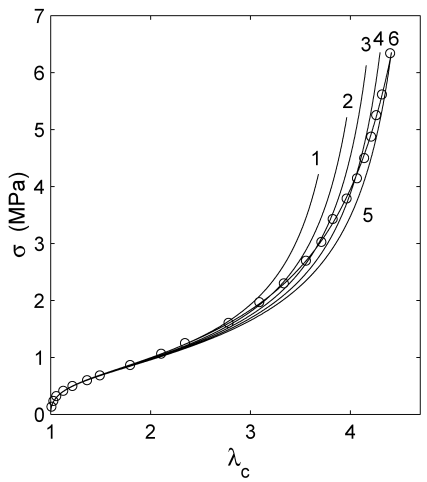

Fig. 4. Dependence of tensile stress on the chain stretch ratio. Points: experimental, NR-1. Curves 1-5: ABGI equation for constant values of λ_{cm}, Table 3, left. The experimental curve 6 drawn through the points coincides with the ABGIL curve ($n = -0.2$, parameter values in Table 3, right).

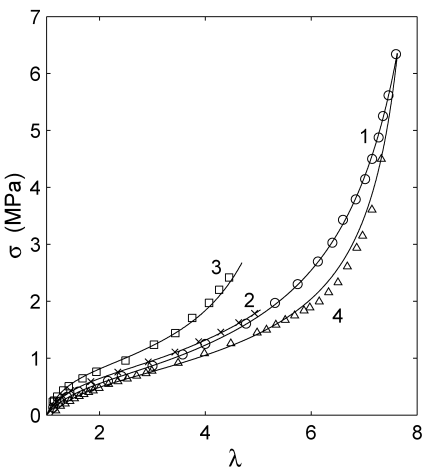

Fig. 5. Dependence of stress on the stretch ratio. Points: experimental, NR-1; circles-UE, crosses-PS, full squares-EBE, triangles-retraction following uniaxial extension. Curves 1 (UE), 2 (PS), 3 (EBE), 4 (retraction) are drawn according to the ABGIL equation, parameter values in Table 3, right.

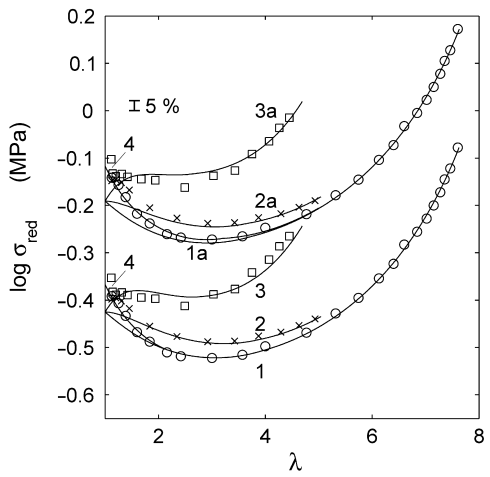

Fig. 6. Dependence of the logarithm of reduced stress on the stretch ratio. Points: experimental, NR-1, circles-UE, crosses-PS, squares-EBE. ABGIL equation, curves 1,2,3: $n = -0.2$, curve 4: $n = -2$. Curves 1a, 2a, 3a ($n = -0.4$), 4a ($n = -2$) and the respective points are shifted vertically by $+0.25$. Parameter values in Tables 1 and 3.

yield the dependence of λ_{cm} ($= N^{1/2}$) on the chain stretch ratio, λ_c. The dependence is compared with Eq. (13) to obtain values of parameters $\lambda_{cm,a}$, $\lambda_{cm,b}$, $\lambda_{c,a}$, $\lambda_{c,b}$, a (Table 3, right) after an overall optimizing procedure is carried out. It should be noted that from the eight parameters contained in the ABGIL equation, only six are truly adjustable; $\lambda_{c,b}$ is determined by the highest strain used in the experiment and $\lambda_{cm,b}$ has practically no freedom of adjustment.

The whole set of the Treloar data is compared with the ABGIL equation in Fig. 3 (Mooney–Rivlin coordinates), in Fig. 5 (linear coordinates) and in Fig. 6 (logarithm of reduced stress vs. stretch ratio). A suitable value found for parameter n ($= -0.2$) is equal to that obtained by Kaliske and Heinrich with their equation [4]. The quality of biaxial data representation obtained with the ABGIL equation at medium and high strains in Figs. 3, 5, 6 is good to very good. On the other hand, systematic data-curve deviations appear at low strains: the zero-strain reduced stress, $\sigma_{red,\lambda=1}(n = -0.2) = 0.367$ MPa, following from the ABGIL equation for $n = -0.2$, is by 12.5% lower than $\sigma_{red,\lambda=1}(n = -2) = 0.429_5$ MPa which follows from the ABGIL equation for $n = -2$ and which is practically equal to a linear extrapolation of experimental reduced stresses in UE, PS, EBE. As a result, at low strains the experimental UE and PS reduced stresses tend to lie above the ABGIL($n = -0.2$) curves (Figs. 3 and 6). On the other hand, at medium and high strains the description of UE and PS data is almost perfect (Figs. 3, 5, 6). Unlike the essentially linear behavior of low-strain experimental data (straight line 5, Fig. 3), the theoretical curve (curve 3 in Fig. 3) calculated for equibiaxial reduced stress goes through a maximum in the region of reciprocal stretch ratios around 0.62. Thus, once again a theoretical curve has to be fitted to a straight-line dependence and the experimental stresses then unavoidably show deviations from the calculated curve. These are not large (only two experimental points deviate more than 5%) but tend to be systematic: positive at small stretch ratios, $\lambda < 1.25$, and negative at medium stretch ratios, $1.5 < \lambda < 2.7$. Such phenomena are obviously due to the approximative form of the W_B function. At high stretches, the EBE point-curve deviations tend to be positive. A slightly lower value of n ($= -0.4$) leads to a higher prediction for the ratio of equibiaxial to uniaxial stress and the positive high-strain deviations are thus practically removed (Fig. 6, curve 3a). This, however, does not solve the problem since the low strain deviations increased. It thus appears that using the generalized invariant-based W_B, a perfect data description cannot, in principle, be achieved and a compromise with a minimum of systematic deviations must always be sought.

Irrespective of these critical remarks, the degree of fit of the ABGIL equation to the Treloar data may be characterized as tolerably satisfactory and, to the best of our knowledge, the most successful so far achieved using a molecularly based constitutive equation.

3.3. Retraction following uniaxial extension

The concept of strain-induced topological changes in the region of high increasing strains implies that on decreasing strain a driving force for topological changes is practically absent [11,26,27]. The highest value of the finite extensibility parameter attained at the highest prestrain may be assumed to remain practically constant on subsequent retraction [11]. The complication arising from the existence of tensile set (ca. 9%), however, must be taken into account and this was done in the manner described previously [11]. In Fig. 5, the retraction data (triangles, read off from Treloar's smooth retraction curve [1]) are described by an ABGI curve based on the foregoing reasoning, with the slightly diminished C_1 parameter only (Table 3; curve 4 in

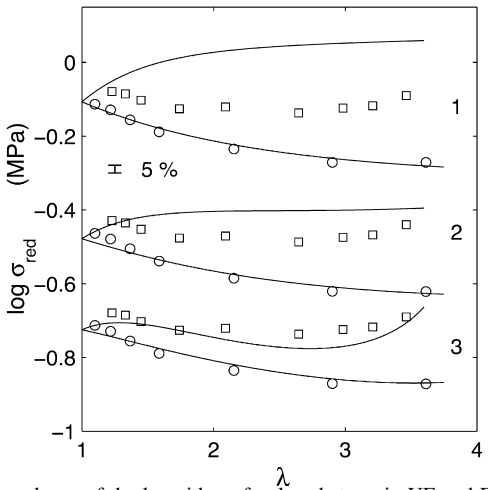

Fig. 7. Dependence of the logarithm of reduced stress in UE and EBE on stretch ratio. Points: experimental, NR-2; circles: UE; squares: EBE. Curves: ABGI equation, parameter values in Table 4. 1-KS, vertical shift: $+0.35$; 2-RP; 3-GD, shift: -0.25.

Table 4
Parameter values of the ABGI equation calculated from experimental biaxial data on the NR-2 network for different values of n

Parameter	KS, KH	RP	KH	KH		HS	GD
n	−1	−1/+1	−0.2	0	0.2	0.5	+1
C_1, MPa	0.094	0.080	0.080	0.074	0.069	0.058	0.045
C_2, MPa	0.080	0.085	0.079	0.087	0.096	0.110	0.120
λ_{cm}	10	6	4.20	3.90	3.70	3.47	3.40
$\sigma_{red,\lambda=1}$	0.349	0.333	0.324	0.328	0.336	0.342	0.335
Δ,[a] %	−5.7	−10.0	−12.5	−11.4	−9.1	−7.5	−9.5
C_2/C_1	0.85	1.06	0.99	1.18	1.39	1.90	2.67

KS Klüppel, Schramm [5]; KH Kaliske, Heinrich [4]; RP Rubinstein, Panyukov [18]; HS Heinrich, Straube [16]; GD Gaylord, Douglas [17].
[a] Δ : see footnote in Table 3

Fig. 5). Similarly as in previous papers [11,26], the quality of description of the lower bound of the hysteresis loop is satisfactory. This result can be regarded as a good support for the concept of finite extensibility parameter increasing with increasing strain and being practically constant on decreasing strain. It has also offered an explanation for the Mullins effect observed in filler-reinforced networks [26].

3.4. Biaxial extension, NR-2

The ABGIL equation has been further experimentally tested using the well-known data of Rivlin and Saunders [1, 28] on a natural rubber network NR-2. The uniaxial stress-stretch ratio dependence was measured up to a stretch ratio not far above the inflexion point and, therefore, data description is possible with a constant value of λ_{cm}; the calculated curve, however, should not be extrapolated too far outside the experimental range. The parameter values obtained with different values of n are given in Table 4.

In Fig. 7, the UE and EBE data plotted in the coordinates of logarithm of reduced stress vs. stretch ratio are compared with three theoretical predictions. A low value of $n = -1$ predicted by Klüppel and Schramm [5] and by Kaliske and Heinrich [4] for $\beta = 1$ gives the best description of the UE dependence but highly overestimates the EBE/UE stress ratio. The Rubinstein and Panyukov theory [23] gives a somewhat better compromise but the predicted EBE/UE stress ratio is still too high. At the other extreme is $n = 1$ predicted by Gaylord and Douglas [22,29] which, however, gives a too low EBE-to-UE stress ratio.

In Fig. 8, the predictions $n = -0.2$ (Kaliske and Heinrich [4], $\beta = 0.2$) and $n = 0.5$ (Heinrich and Straube [21]) are tested in the plot used by Rivlin and Saunders [1,28], i.e. as a dependence of uniaxial extension and compression reduced stress on the reciprocal stretch ratio with a change of scale at $1/\lambda = 1$. In this type of plot, the point-curve deviations at low extension and compression strains are visually enlarged and accentuated while in the high-extension region they are somewhat suppressed. The same type of plot is used in Fig. 9 for the ABGI curve with $n = +0.2$ and this apparently gives an optimum data representation. With the exception of the low-strain region, the degree of fit of the ABGI($n = 0.2$) curve to the data at stretch ratios in the regions $\lambda_{UC} = 0.4$ to 0.08 and $\lambda_{UE} = 1.5$ to 3.6 is very good and the best so far found in the tests of molecular elasticity theories [18,30].

3.5. General biaxial data on networks IR and NR-3

In the paper of Kawabata et al. [31], stresses σ_1, σ_2, measured on an isoprene rubber network are tabulated as functions of λ_2 for different constant values of λ_1. The experimental dependences of log σ_1 on λ_2 are shown in Fig. 10 (points) and compared with Eqs. (6)–(8),(13) (curves). Parameter sets (Table 5) with $n = -0.2$ and $n = +0.2$, respectively, give approximately the same quality of data description, with only a few point-curve deviations in the region from 5 to 8%. The dependences of log σ_2 on λ_2 (not

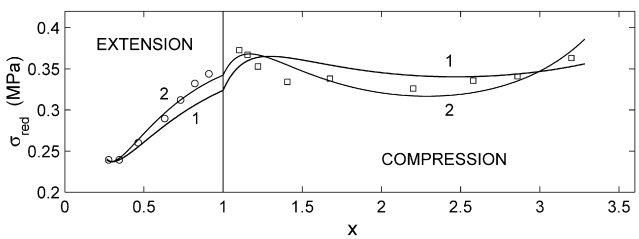

Fig. 8. Dependence of reduced stress in UE and in uniaxial compression UC on reciprocal stretch ratio. Points: experimental, NR-2; circles: UE; squares: UC. Curves: ABGI equation, parameter values in Table 4. $1 - n = -0.2$; $2 - n = +0.5$. Note the change in scale at $x = 1$. For $x < 1$, $1/\lambda_{UE} = x$; for $x > 1$, $1/\lambda_{UC} = 5x - 4$.

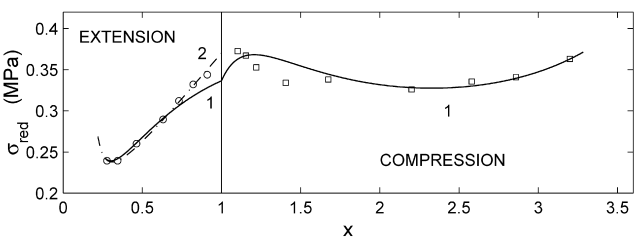

Fig. 9. Dependence of reduced stress in UE and UC on reciprocal stretch ratio. Points: experimental, NR-2; circles: UE; squares: UC. Curves: ABGI equation. $1 - n = 0.2$, parameters in Table 4; $2 - n = -2$, for UE data only, parameters in Table 1. Note change of scale at $x = 1$. For $x < 1$, $1/\lambda_{UE} = x$; for $x > 1$, $1/\lambda_{UC} = 5x - 4$.

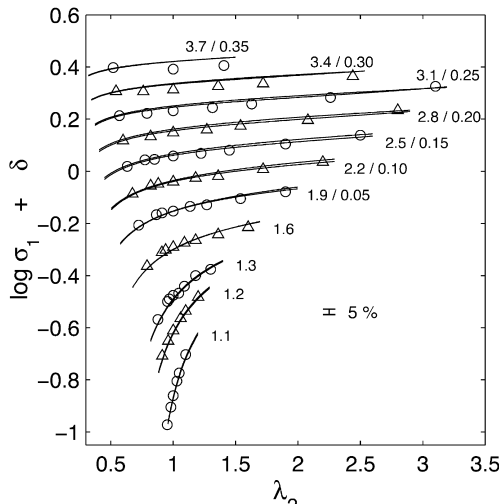

Fig. 10. Dependences of log σ_1 on λ_2 for different constant values of λ_1. Points: experimental, IR. Curves: ABGIL equation, parameter values in Table 5. Numbers on the curves indicate λ_1/vertical shift.

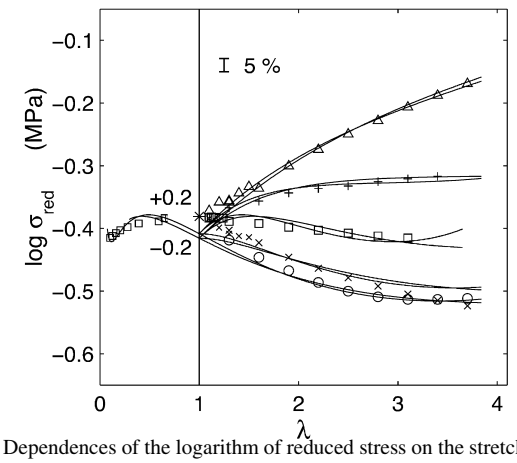

Fig. 11. Dependences of the logarithm of reduced stress on the stretch ratio for different values of b. Points: experimental, IR. Curves: ABGI equation, parameter values in Table 5. log $\sigma_{1,red}$: circles, $b = -1$; lying crosses, $b = 0$; squares, $b = 2$, $\lambda > 1$: EBE, $\lambda < 1$: UC. log $\sigma_{2,red}$: triangles, $b = 0$; standing crosses, $b = 1$. Asterisk: extrapolated zero-strain reduced UE stress.

shown here) are described by the ABGI curves even better than the dependences of log σ_1 on λ_2. With the lower value of n used, the deviations in the low-strain region become more significant (Table 5). Fig. 11 shows dependences of the logarithm of reduced stresses $\sigma_{1,red}(b = -1, 0, 2)$ and $\sigma_{2,red}(b = 0, 1)$ on stretch ratio λ (subscript 1 is omitted) in comparison with the ABGI curves drawn for parameters given in Table 5. With the exception of equibiaxial extension (and its equivalent, uniaxial compression), only data for $\lambda > 1.24$ are plotted because with λ decreasing from 1.24 to 1.04 (not shown here), the reduced stresses calculated from the Kawabata et al. data for $b = -1$ and 0 show a pronounced tendency to rapidly decrease below the respective values attained at $\lambda = 1.24$. Moreover, the reduced transversal pure shear stress, $\sigma_{2,red}(b = 0)$, becomes smaller than the reduced longitudinal pure shear stress, $\sigma_{1,red}(b = 0)$ and this does not seem to be reasonable. Although Kawabata et al. believe that their data even in the very low strain region are reliable, one cannot exclude that the phenomena described may well be artefacts resulting from an even small uncertainty in the determination of the stretch ratio at small strains [11,26]. We have found that a very small correction of the stretch ratio values (by a constant of some 0.001–0.003 in a given series of measurements) can remove the effect and make the reduced stresses approach the value obtained by extrapolation of UE, EBE data in Fig. 2, shown in Fig. 11 as an asterisk. It should also be recalled that pure shear measurements of Treloar (Figs. 3 and 6) do not show any decreasing trend in the reduced stress with strain decreasing to zero. We have read off several low-strain values of pure shear stresses from Fig. 3 of Kawabata et al.; the reduced stresses calculated from them do not show any anomalous decrease at low strains, and they are included in our Fig. 11. One more discrepancy is seen in Fig. 11: the reduced longitudinal pure shear stress, $\sigma_{1,red}(b = 0)$, becomes smaller than the reduced uniaxial stress $\sigma_{1,red}(b = -1)$ at high stretch ratios. This is contrary

Table 5
Parameter values of the ABGIL equation calculated from experimental biaxial data on IR and NR-3

Parameters	IR		NR-3	
n	−0.2	+0.2	−0.2	+0.2
C_1, MPa	0.126_5	0.108	0.159	0.150
C_2, MPa	0.064	0.084	0.063	0.078
$\lambda_{c,a}$	–	–	1.795_1	1.688_6
$\lambda_{cm,a}$	–	–	3.709_1	3.537_3
$\lambda_{c,b}$	–	–	2.828_6	2.826_4
$\lambda_{cm,b}$	7.2[a]	4.6[a]	3.892_6	3.795_1
a	–	–	1.35	1.60
$\sigma_{red,\lambda=1}$	0.384	0.390	0.459	0.472
Δ, %	−9.2	−6.6	−12.1	−9.7
C_2/C_1	0.51	0.78	0.40	0.52

Δ : see footnote in Table 3.
[a] λ_{cm}.

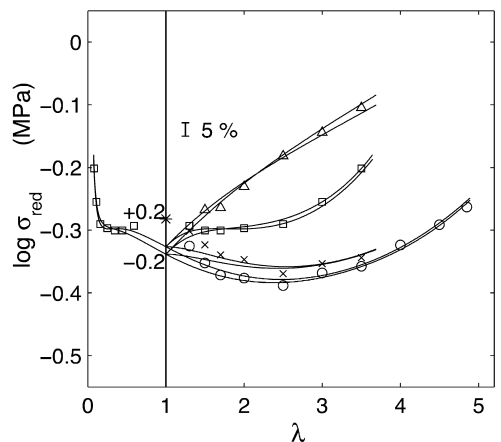

Fig. 12. Dependences of the logarithm of reduced stress on the stretch ratio for different values of b. Points: experimental, NR-3. Curves: ABGIL equation, parameter values in Table 5. log $\sigma_{1,red}$: circles, $b = -1$; crosses, $b = 0$; squares, $b = 2$, $\lambda > 1$: EBE, $\lambda < 1$: UC. log $\sigma_{2,red}$: triangles, $b = 0$. Asterisk: extrapolated zero-strain reduced UE stress.

to theoretical expectations and to the Treloar data in Figs. 3 and 6, where $\sigma_{1,red}(b = 0)$ remains larger than $\sigma_{1,red}(b = -1)$ in the whole strain range up to high stretch ratios in pure shear.

Irrespective of the experimental discrepancies just mentioned, it should be stressed that the Kawabata et al. measurements yield the best and most valuable biaxial stress–strain data in a very wide range of stretch ratios, which, moreover, are not complicated by crystallization effects. The data representation by the ABGI equation is very good and the point-curve deviations are of the same type as found for networks NR-1 and NR-2, with only very few higher than 5%. Of the two values of n tested, the higher one, $n = +0.2$, gives a better representation of the uniaxial compression (equibiaxial extension) data and less significant deviations at low strains. However, to obtain a good fit to high-strain data, the finite extensibility parameter must be adjusted to a value leading to a rather early upturn of equibiaxial reduced stress.

Experimental data of James et al. [32] on the NR-3 network showing pronounced finite extensibility effects, are successfully represented by the ABGIL equation (Fig. 12). Similarly to the data on the IR network (Fig. 11), the low-strain deviations obtained with $n = +0.2$ are less significant than those with $n = -0.2$ and the uniaxial compression (equibiaxial extension) data are somewhat better represented.

3.6. Parameter values

The value of $n = -0.2$ obtained for the Treloar network NR-1 seems to be well substantiated by the good data representation up to high strains. It agrees with the n estimated by Kaliske and Heinrich, lying in the range predicted by their theory [4]. With the remaining three networks, the range of applied deformations was narrower and since the W_B function is not able to give a strictly accurate description of the experimental low-strain behavior, an unequivocal value of n is difficult to assign. Rather, possible values of n are found to lie in the range from -0.2 to $+0.2$. For values of n from 0 to $+0.2$, no theoretical prediction is available. It should be noted that a comparison [33] of the Kaliske-Heinrich equation with the extension/compression data obtained on two peroxide-crosslinked natural rubber networks at low strains (with $\delta = 0$) gave estimates of $\beta (= -n) \sim 0$. Equibiaxial and uniaxial extension measurements [5] on a natural rubber network are claimed to support the value of $\gamma = 1/2$ ($n = -1$). However, an inspection of Fig. 6 in Ref. [5] reveals that the ratio of experimental stresses in equibiaxial and uniaxial extension is unusually high (1.67 at $\lambda = 2$), much higher than are the ratios 1.33–1.44 which were found on the four networks explored in the present paper. Before this difference is explained, the data in Ref. [5] are to be treated with caution and should not serve as an argument in favour of $n = -1$.

The ABGIL($n = -2$) elastic constants C_1, C_2, based on UE data alone (Table 1) are almost equal to those obtained from comparisons of experimental stress-elongation measurements with the Mooney–Rivlin equation. Systematic studies of the relations between the network structure and Mooney–Rivlin parameters were already made several decades ago, e.g. [34–37]. The following conclusions were derived: the modulus component $2C_1$ contains contributions from both chemical crosslinks and trapped entanglements of a 'stable', i.e. junction-like nature; the modulus component $2C_2$ stems from sliding ('labile') entanglements; for natural rubber networks, the contributions of stable and labile entanglements to the modulus (after extrapolation to networks without free chain ends) were found to be virtually equal [37]. In the framework of the tube model [38], and similarly to the earlier findings based on the Mooney-Rivlin equation and UE data, entanglements are found to contribute to the crosslink part of the modulus, i.e. to behave in a junction-like manner, presumably with a somewhat lower elastic efficiency (lower microstructure factor) than the crosslinks. The entanglement spacing (tube diameter) determines the topological constraint modulus G_e ($= 2C_2$) and the inextensibility parameter δ is given not only by the entanglement spacing as in the earlier tube treatments but also by the trapping factor T_e [38], i.e. by the concentration of crosslinks, as well, This prediction is more in line with our view given above (locking chain stretch ratio $\sim N^{1/2}$, with N given by both crosslinks and entanglements contributing to C_1).

In order to get a simultaneous description of the UE and EBE data or, a representation of the biaxial extension data generally, the value of the exponent n in the ABGIL equation must be increased from -2 (which is optimum for UE data) into the -0.2 to $+0.2$ region. This leads to a decrease in the zero-strain reduced modulus by some 9–12% and to a decrease in C_2 by 20–50% while the C_1 values tend to show some increase (0–20%, Tables 1, 3–5).

Contribution of trapped entanglements to the concentration of elastically effective network junctions (to C_1) may be expected to be accompanied by a decrease in the number N, of statistical segments in the effective network chain, i.e. by a decrease in the network mesh size and in the limiting extensibility [5].

The idea that at high strains the junction points between molecules in the actual rubber may not be as definite as the theory requires was taken into account by Rivlin and Saunders more than fifty years ago [28]. They wrote: 'There may be effective junction points akin to entanglement cohesions, which may break down under certain states of strain'. Wu and van der Giessen [39] discussed the possibility that entanglements are being pulled out during deformation which would mean that the concentration of network chains during deformation decreases while the number of segments per chain increases, thus reducing the stiffness of the network. They conclude that this aspect

absolutely requires further study. Our concept of strain-induced increase in the network mesh size is a certain development of these ideas. It assumes that at high strains even 'stable' entanglements contributing to C_1 may be forced to slide, with a resulting increase in the network mesh size. It should be recalled that in the slip-link model the sliding entanglements contribute to the high-strain hardening in a similar manner as crosslinks.

4. Conclusion

A four-parameter constitutive equation given by a combination of the Langevin-theory-based Arruda–Boyce equation [3] with the constraint term based on the first invariant of the generalized deformation tensor [1,18] gives a satisfactory description of biaxial stress–strain data obtained on homogeneous networks of natural and isoprene rubbers. The experiment-curve deviations are for the most part smaller than 5%. With the exception of the low-strain regions, the reduced uniaxial and pure shear stress–strain dependences are described very well. The reduced stress in equibiaxial-extension (uniaxial compression) generally shows greater point-curve deviations which tend to be systematic in some stretch regions.

For the description of high-strain data, the previously used concept [11] of a strain-dependent finite extensibility parameter has been successfully applied. Based on the knowledge of the stress–strain dependence on increasing extension, a reasonable prediction for the subsequent retraction behavior of the natural rubber network is obtained [11,26,27].

For the hydrocarbon rubber networks studied, parameter n in the constraint term has been found to have values in the -0.2 to $+0.2$ range. Thus, in some cases it tends to lie above the highest value ($n = 0$) expected by the Kaliske and Heinrich theory [4]. It will be shown in the second part of this paper, using networks of other polymers, that the tendency of n to assume positive values is rather general.

The ABGIL equation offers a reasonable compromise between the simplicity of equation and quality of description and it gives, to the best of our knowledge, the most accurate data representation so far achieved using a molecularly based equation.

Acknowledgements

The authors are greatly indebted to the Grant Agency of the Czech Republic for financial support of this work within the grant project No. 104/00/1311 and to the Grant Agency of the Academy of Sciences of the Czech Republic for financial support within the grant project No. A4050008.

Appendix A

In the Arruda and Boyce theory [3], the *low-strain* reduced stress divided by the shear modulus, σ_{red}/G, is equal to unity if N is high. With decreasing N (increasing inextensibility), σ_{red}/G is predicted to increase for all geometrical modes, i.e. the contribution of finite extensibility to the stress is always positive. In the tube theories of Kaliske and Heinrich [4] and of Klüppel and Schramm [5], σ_{red}/G calculated on the basis of the crosslink term is given by the relation:

$$\sigma_{red}/G = \frac{1-\delta^2}{(1-\delta^2(I-3))^2} - \frac{\delta^2}{1-\delta^2(I-3)}$$

δ is the inextensibility parameter, I is given by Eq. (8). For a zero strain ($I = 3$), $\sigma_{red}/G = 1 - 2\delta^2$. This leads to the prediction that with increasing inextensibility, σ_{red}/G should *decrease* below unity. The contribution of finite extensibility to the stress is thus predicted to be *negative*, which does not seem to be physically realistic. For large $\delta > 0.707$ and low strains, even a negative stress is predicted. σ_{red}/G becomes higher than unity not before I exceeds 4 ($\lambda_{UE} > 1.67$, $\lambda_{EBE} > 1.36$).

Appendix B

NR-1 (Treloar [9]), natural rubber crosslinked with a high concentration of sulfur to suppress orientational crystallization (RSS 100, S 8, vulcanized at 147 °C for 3 h). Equilibrium measurements on prestrained specimens. Equibiaxial extension data obtained from inflation of a rubber sheet, 20 °C.

NR-2 (Rivlin and Saunders [28]), sulfur-accelerator crosslinked natural rubber (RSS 100, S 2, 2,2′-dithiobis-(benzothiazole) 1, ZnO 2, stearic acid 0.5, vulcanized at 141 °C for 30 min). Inflation of a rubber sheet.

NR-3 (James et al. [32]), sulfur-accelerator crosslinked natural rubber (NR 100, S 2.5, *N*-cyclohexylbenzothiazole-2-sulfenamide 0.5, ZnO 5, stearic acid 2, vulcanized at 135 °C for 50 min). The test piece was stress-softened by stretching ten times to the maximum deformation. The stretching force was recorded after 5 min relaxation at a given strain. Biaxial tensile test apparatus.

IR (Kawabata et al. [31]), sulfur-accelerator crosslinked isoprene rubber (IR 100, ZnO 5, S 2, 2,2′-dithiobis(benzothiazole) 1, tetramethylthiuram disulfide 0.1, stearic acid 2). Data were taken on pre-strained specimens under equilibrium conditions. Biaxial tensile test apparatus.

References

[1] Treloar LRG. The physics of rubber elasticity, 3rd ed. Oxford: Clarendon Press; 1975 (Chapters 5,10,11).

[2] Erman B, Mark JE. Structure and properties of rubberlike networks. New York: Oxford University Press; 1997 (Chapters 2–5,10).
[3] Arruda EM, Boyce MC. Mech Phys Solids 1993;41:389–412.
[4] Kaliske M, Heinrich G. Rubber Chem Technol 1999;72:602–32.
[5] Klüppel M, Schramm J. Macromol Theory Simul 2000;9:742–54.
[6] James HM, Guth E. J Chem Phys 1943;11:455–81.
[7] Boyce MC, Arruda EM. Rubber Chem Technol 2000;73:504–23.
[8] Flory PJ, Erman B. Macromolecules 1982;15:800–6.
[9] Treloar LRG. Trans Faraday Soc 1944;40:59–70.
[10] Edwards SF, Vilgis TA. Polymer 1986;27:483–92.
[11] Meissner B. Polymer 2000;41:7827–41.
[12] Meissner B, Matêjka L. Polymer 2002;43:3803–9.
[13] Kawamura T, Urayama K, Kohjiya S. Macromolecules 2001;34: 8252–60.
[14] Kawamura T, Urayama K, Kohjiya S. J. Polym Sci. Part B: Polym Phys 2002;40:2780–90.
[15] Urayama K, Kawamura T, Kohjiya S. Macromolecules 2001;34: 8261–9.
[16] Urayama K, Kawamura T, Kohjiya S. J Chem Phys 2003;118:5658–64.
[17] Meissner B. In preparation.
[18] Heinrich G, Straube E, Helmis G. Adv Polym Sci 1988;85:33–87.
[19] Ogden RW. Proc R Soc London. Ser A 1972;326:565–84.
[20] Blatz PJ, Sharda SC, Tschoegl NW. Trans Soc Rheol 1974;18: 145–61.
[21] Heinrich G, Straube E. Acta Polym 1983;34:589–94.
[22] Gaylord RJ, Douglas JF. Polym Bull 1987;18:347–54.
[23] Rubinstein M, Panyukov S. Macromolecules 1997;30:8036–44.
[24] Mooney M. J Appl Phys 1940;11:582–92.
[25] Rivlin RS. Philos Trans R Soc London. Ser A 1948;241:379–97.
[26] Meissner B, Matêjka J. Polymer 2000;41:7749–60.
[27] Meissner B, Matêjka L. Polymer 2001;42:1143–56.
[28] Rivlin RS, Saunders DW. Philos Trans R Soc London Ser A 1951; 243:251–88.
[29] Gaylord RJ, Douglas JF. Polym Bull 1990;23:529–33.
[30] Gottlieb M, Gaylord RJ. Polymer 1983;24:1644–6.
[31] Kawabata S, Matsuda M, Kawai H. Macromolecules 1981;14:154–62.
[32] James AG, Green A, Simpson GM. J Appl Polym Sci 1975;19:2033–58.
[33] Roland CM, Mott PH, Heinrich G. Comput Theoret Polym Sci 1999; 9:197–202.
[34] Mullins L. J Polym Sci 1956;19:225–36.
[35] Moore CG, Watson WF. J Polym Sci 1956;19:237–54.
[36] Meissner B. J Polym Sci Part C 1967;16:781–92.
[37] Meissner B, Klier I, Kuchaîík S. J Polym Sci, Part C 1967;16:793–804.
[38] Klüppel M, Menge H, Schmidt H, Schneider H, Schuster RH. Macromolecules 2001;34:8107–16.
[39] Wu PD, van der Giessen E. Mech Phys Solids 1993;41:427–56.